Available online at www.sciencedirect.com
ScienceDirect
Journal of Power Sources 177 (2008) 56–60
JOURNAL OF POWER SOURCES
www.elsevier.com/locate/jpowsour

Short communication

Dynamic conducting effect of WO_3/PFSA membranes on the performance of proton exchange membrane fuel cells

Jinyan Yang, Yongliang Li, Yueqiang Huang, Jianying Liang, Pei Kang Shen *

State Key Laboratory of Optoelectronic Materials and Technologies, School of Physics and Engineering, Sun Yat-Sen University, Guangzhou 510275, PR China

Received 2 October 2007; received in revised form 8 November 2007; accepted 8 November 2007
Available online 17 November 2007

Abstract

The homogenous proton conducting WO_3/PFSA membranes are prepared based on a dynamic conducting concept, that is, the resistance of the membrane can be reduced during the fuel cell operation due to the formation of the conducting hydrogen tungsten bronzes. The novel membranes are characterized by different techniques. The results proved that the resistances of the WO_3-containing membranes in single fuel cells measured by in situ AC impedance spectroscopy during the operation are significantly lower than that of the single fuel cell using Nafion® 112 membrane. It is revealed that the performances of the single fuel cells with WO_3/PFSA membranes are superior to that of the single cell with Nafion® 112 membrane.

Keywords: Proton exchange membrane; Fuel cells; Conductivity; WO_3; AC impedance spectroscopy

1. Introduction

Perfluorosulfonic acid (PFSA) membranes are commonly used for the polymer electrolyte membrane fuel cells (PEMFCs) [1]. PFSA membranes are relatively strong and stable in both oxidative and reductive environments since the structure of PFSA is based on polytetrafluoroethylene (PTFE) backbone. The conductivity of a well-humidified PFSA membrane can be as high as 0.2 S cm^{-1}. However, PFSA membrane must be kept hydrated to retain proton conductivity. Water loss is anticipated to have two negative impacts on cell performance. One is that the membrane proton conductivity is decreased and the second is that the shrinkage of the membrane which is expected to degrade the membrane–catalyst interface. As we known that the main contribution to cell resistance is due to the ionic resistivity of the electrolyte (membrane). One way to improve the water retention property and substantially the conductivity of the membrane is to make inorganic/organic composite [2–4]. The fact is that the conductivities of these inorganic/organic composite membranes are usually reduced with the increase in the content of inorganic additives [5–9]. There are only few reports showing the increase in the conductivity of the PFSA membranes with the cooperation of the inorganic materials [10,11]. In electrochemistry, the increase in the membrane conductivity is highly effective to increase the cell voltage output.

Our idea on the synthesis of high conducing membranes is to add special additives into PFSA ionomer to prepare homogeneous composite membrane. These additives can be transferred to conducting form during the fuel cell operation, that is, the membrane possesses a dynamic characteristic to increase the conductivity and consequently the cell performance. Herein, we report the synthesis of WO_3/PFSA membranes. The basic consideration is that hydrated WO_3 can keep the membrane moistened to retain the conductivity [12]. Moreover, WO_3 can be transferred to conducting hydrogen tungsten bronze during the hydrogen oxidation by a spill-over effect to increase the conductivity dynamically [13–17].

2. Experimental

2.1. Membrane preparation

The WO_3/PFSA membranes were prepared by recasting the perfluorosulfonic acid ionomer dispersion (EW1000, 10 wt%

* Corresponding author. Tel.: +86 20 84036736; fax: +86 20 84113369.
E-mail address: stsspk@mail.sysu.edu.cn (P.K. Shen).

0378-7753/$ – see front matter © 2007 Elsevier B.V. All rights reserved.
doi:10.1016/j.jpowsour.2007.11.022

PFSA in DMF, Dongyue Group, China) and the tungsten trioxide precursor solution. Tungsten-containing solution was prepared by dissolving 2.5 g tungsten powder in 100 ml aqueous solution containing 50 ml 30% (v/v) H_2O_2, 25 ml isopropyl alcohol and 25 ml distilled–deionized water. The reaction solution was put steadily for 24 h, then, a Pt foil was used to decompose the excessive H_2O_2. After filtering the solution, a homogenous tungsten-containing precursor solution was obtained.

A quantity of the tungsten-containing solution and the PFSA dispersion were mixed together and stirred at room temperature for 3 h. The mixture was recast on a flat glass plate and then treated by programmed heating in an oven at 50 °C for 30 min and followed at 120 °C for 2 h and at 135 °C for 6 h. The thickness of these membranes was controlled at about 50 um.

2.2. Characterization of the membranes

2.2.1. Scanning electron microscopy (SEM) and energy-dispersive X-ray spectroscopy (EDX) analysis

The surface and the cross-sectional morphologies of the composite membranes were examined on a Quaunta 400F (FEI, Netherlands)/INCA/HKL thermal field emission environmental scanning electron microscope (FEESEM). For the cross-sectional SEM samples, the membranes were freeze-fractured in liquid N_2. A low voltage (5 kV) was operated to lower the electron beam energy and avoid damage to the membranes. The distributions of the tungsten element along the membrane surface and cross-section were detected by EDX.

2.2.2. Water content of the membranes

The membranes were dried under vacuum at 80 °C for 12 h and weighted prior to testing. The membranes were immersed in deionized water at room temperature for 8 h. The external water was carefully wiped off with a filter paper before weighting again. Water uptake differences between wet and dry weights of the samples were determined by the following equation:

$$W\% = \frac{W_1 - W_0}{W_0} \times 100\%$$

Here W_0 and W_1 are the mass of the membrane before and after water absorption.

2.2.3. Thermogravimetric analysis (TGA)

Thermogravimetric analysis was carried out to detect the temperature-programmed decomposition of the membrane using TG 209 (NETZSCH Corporation, Germany) at a rate of 10 °C min^{-1} under N_2 atmosphere. The membrane samples were in hydrate state before measurement.

2.2.4. Proton conductivity measurement

Proton conductivity of the membrane was determined by a two-probe AC impedance method using IM6e electrochemical station (Zahner-Electrik, Germany) with a frequency range from 1 Hz to 1 MHz. The AC signal was 10 mV. Membrane samples were cut into strips of 1 cm wide and 4 cm long. The conductivity cell was place in a stainless steel chamber where the temperature and humidity can be controlled. To maintain a more accurate humidity for impedance measurement, the samples were equilibrated in the chamber at lest for 12 h before the impedance spectra were recorded [18–20].

2.3. Single PEM fuel cell test

2.3.1. Preparation of membrane electrode assembly (MEA)

The membrane electrode assembly (MEA) was prepared by hot pressing the anode and cathode to the membrane at 10 MPa and 135 °C for 3 min. Carbon paper (180 μm, Toray Industries Inc., Japan) was used as current collector. The gas diffusion layer on the carbon paper was composed of 20 wt% PTFE and 1.0 mg cm^{-2} carbon powder (Vulcan XC-72R, Cabot Corp., USA). The active surface area of the MEA was 1.5 cm × 1.5 cm with 0.5 mg cm^{-2} Pt (50 wt%Pt/C, Johnson Matthey) both in anode and cathode. To protect the electron-conducting path by hydrogen tungsten bronze formed in the membrane, 5% Nafion suspension (DuPont, USA) was sprayed onto the cathode side of membrane to form a polymer coating. The MEA was assembled to a single fuel cell using gold-coated stainless steel as the end plates.

2.3.2. Single fuel cell performance

Performances of the single fuel cells were evaluated by recording the current density vs. cell voltage polarization curves using the Arbin fuel cell test system (Arbin Instrument, USA). The singe fuel cell was operated with dry air and hydrogen at atmospheric pressure from 30 to 60 °C. The flow rate of air was 800 ml min^{-1} and H_2 was 1.5× stoich. Polarization curves were recorded after the single fuel cell was activated.

2.3.3. In situ AC impedance spectroscopic analysis

AC impedance spectroscopic method was used to analyze the dynamic characteristic of the WO_3/PFSA membranes under fuel cell operation. In situ impedance spectra were recorded under constant current density on IM6e electrochemical station. The IM6e instrument was connected to the fuel cell with the counter and reference electrodes contacting to the anode and work electrode contacting to the cathode [21–23].

3. Results and discussion

Fig. 1 shows the SEM micrographs of the surface and cross-section of 15 wt% WO_3/PFSA membrane and their corresponding EDX thermal field emission images for tungsten element. The results show that the surface of the composite membrane is even and dense. The EDX mapping images both along the surface and cross-section clearly show that the tungsten element is uniformly distributed in the composite membranes.

The thermal properties of the WO_3/PFSA membrane were analyzed by the TG-DTG measurements along with the Nafion® 112 membrane for comparison. The sharp DTG peak at 300–400 °C as shown in Fig. 2 is associated with the decomposition of the sulfonic acid groups (SO_3H) from the PFSA membranes [24]. At temperatures over 400 °C, mass loss for the ether side chains and Teflonic polymer backbone are observed. Contrast with the sulfonate loss peak of a pure Nafion membrane,

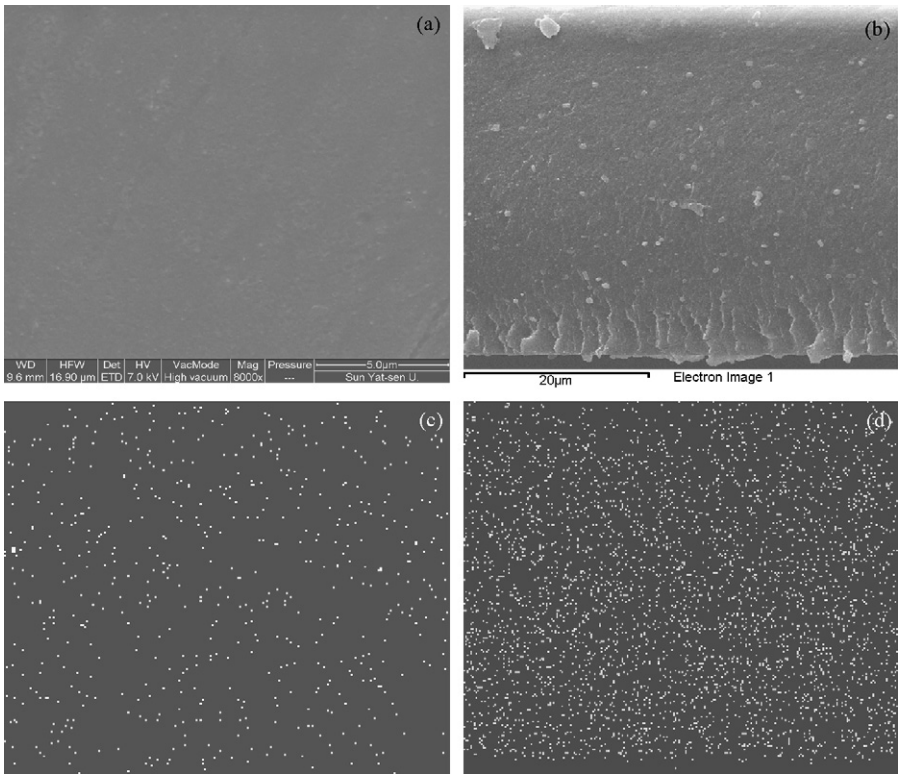

Fig. 1. SEM micrographs of (a) the surface and (b) cross-section of a 15 wt% WO_3/PFSA membrane; EDX mapping along (c) the surface and (d) the cross-section.

which shows a large temperature spread for this decomposition, the TG-DTG response changes dramatically upon addition of a WO_3 component to the membrane. These data suggest that WO_3 catalytically removes the Nafion sulfonate groups above 300 °C, a process that is possible only if there is a specific molecular contact between the sulfonate groups and the WO_3 surface.

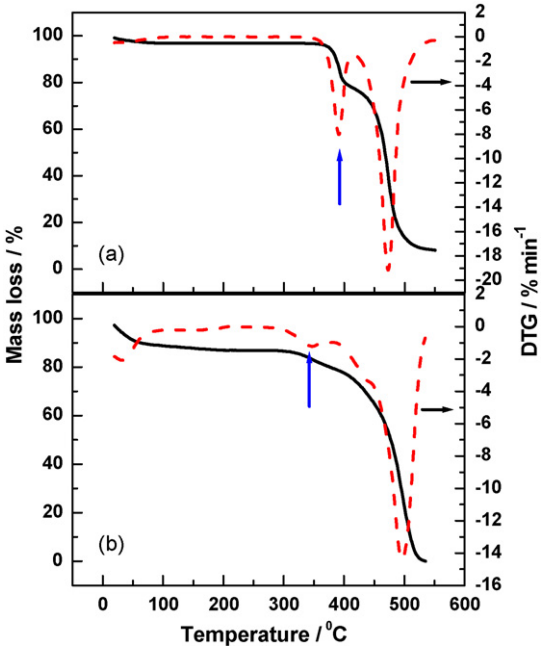

Fig. 2. Thermal gravimetric spectra of (a) 8 wt% WO_3 and (b) Nafion® 112 membranes.

Water uptake for various membranes is summarized in Table 1. It shows that the water contents in composite membranes are higher than that of Nafion® 112 membrane. This might be attributed to the hydrophilic property of WO_3 particles. It should be noticed, however, that the temperatures for the decomposition of the sulfonic acid groups is increased for the WO_3/PFSA membrane compared with that of the pure Nafion® 112 membrane, indicating the enhancement in the stability of the sulfonic acid groups. The results suggest that incorporation of WO_3 not only improves the water management characteristics of a PFSA membrane but also enhances the membrane stability operating at elevated temperature. Conductivity measurements on freestanding membranes indicate that the composite membrane is slightly less conductive than a pure Nafion membrane (Fig. 3) as we recognized.

Single fuel cells were assembled to investigate the dynamic characteristics of the WO_3/PFSA membranes. Fig. 4 shows the performance of the single cells with 8 wt% WO_3/PFSA, 15 wt% WO_3/PFSA and Nafion® 112 membranes at 45 °C under dry

Table 1
Charge transfer resistances of Nafion® 112 and 15 wt% WO_3/PFSA membranes at different polarization current densities

Current density (mA cm^{-2})	Charge transfer resistance (Ω)	
	Nafion® 112	15 wt% WO_3/PFSA
50	0.535	0.490
150	0.231	0.230
300	0.133	0.131
450	0.094	0.095

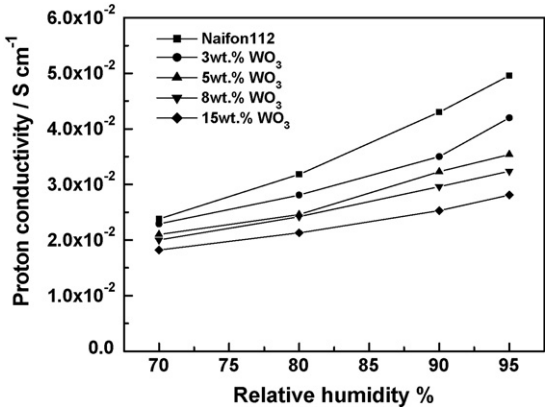

Fig. 3. Proton conductivity at 30 °C as a function of relative humidity for different membranes.

H_2/air operation conditions. The performances of the single cells with WO_3/PFSA membranes are superior to that of the single cell with Nafion® 112 membrane. Over 30% improvements in the output power are achieved. It has also been noticed that the performance of the single cells with WO_3/PFSA membranes is even better operating at higher current densities. It is obvious that the voltage declines down to lower values more quickly at higher current densities for the single cell with Nafion® 112 membrane. The power density output shows the similar tendency.

The dynamic conductivities of the WO_3/PFSA membranes were monitored by in situ AC impedance spectroscopy. The impedance spectra were measured under polarization of the fuel cell at different current densities. In situ AC impedance spectra of 8 wt% WO_3/PFSA, 15 wt% WO_3/PFSA and Nafion® 112 membranes in single fuel cells operating at 150 mA cm^{-2}, 45 °C are compared in Fig. 5. It is obvious that the resistances of the WO_3-containing membranes are lower than that of the Nafion® 112 membrane.

Fig. 6 shows the AC spectra of the membranes in fuel cells operating at different galvanostatic current densities. It can be seen that the omhic resistances of 15 wt% WO_3/PFSA membrane are lower than that of Nafion® 112 membrane at corresponding current densities. Table 1 summarizes the charge

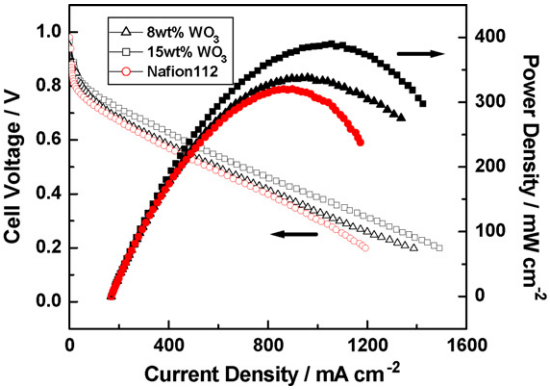

Fig. 4. Current-voltage curves for single fuel cells with different membranes at dry H_2/air. T_{cell} = 45 °C, $P_{H_2} = P_{air}$ = 0.025 MPa, 1.5× stoich for H_2 and 800 ml min^{-1} for air, scan rate: 10 mV s^{-1}. (△) 8 wt% WO_3/PFSA membrane, (□) 15 wt% WO_3/PFSA membrane and (◇) Nafion® 112 membrane.

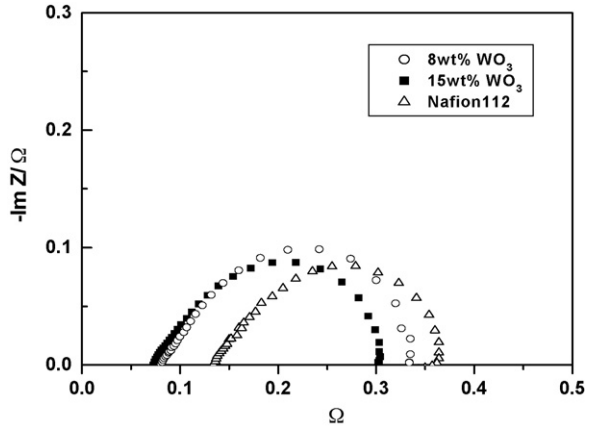

Fig. 5. Comparison of the in situ AC impedance spectra of the single fuel cells with different membranes under dry H_2/air at galvanostatic current density of 150 mA cm^{-2}, T_{cell}: 45 °C.

transfer resistances calculated from the semicircle on the real impedance axis both for Nafion® 112 and 15 wt% WO_3/PFSA membranes against current density. As we expected that the charge transfer resistance degreases with the increase in the current density. However, two sets data are very close, indicating that two membranes have the similar charge transfer behavior. This further proves that the improvement in the fuel cell performance by using WO_3/PFSA membrane is mainly due to the reduction of the ohmic drop of the membrane.

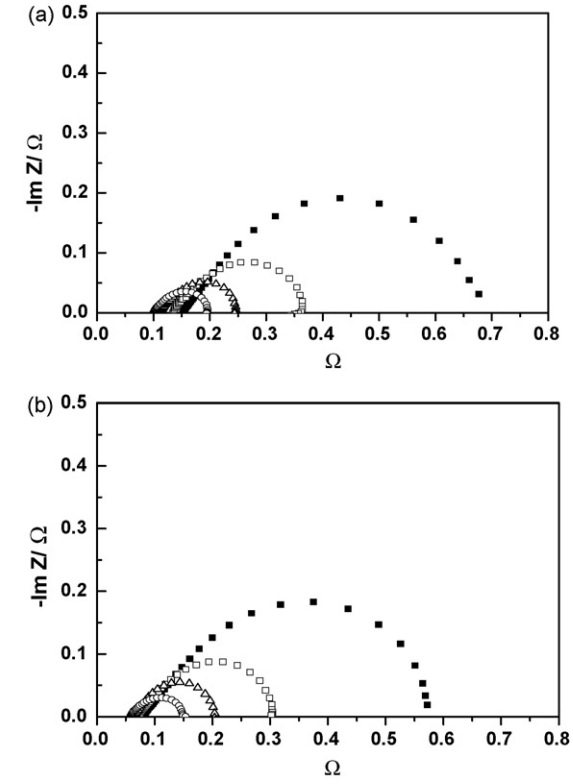

Fig. 6. Impedance spectra of single fuel cells at different current densities with dry H_2/air: (a) Nafion® 112 and (b) 15 wt% WO_3/PFSA membranes. (■) 50 mA cm^{-2}, (□) 150 mA cm^{-2}, (△) 300 mA cm^{-2} and (◯) 450 mA cm^{-2}. T: 45 °C, frequencies: 0.05 Hz to 10 KHz.

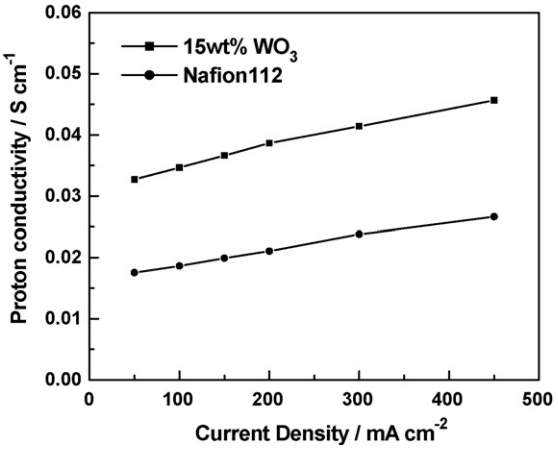

Fig. 7. Plots of the proton conductivity of 15 wt% WO_3/PFSA membrane and Nafion® 112 membrane against the cell discharging current densities.

Fig. 7 shows the plots of the proton conductivities of the 15 wt% WO_3/PFSA membrane and Nafion® 112 membrane against current densities based on the AC impedance spectroscopic results. It can be seen that the conductivities of the 15 wt% WO_3/PFSA membrane are higher than that of Nafion® 112 membrane in measured current density range. The higher the discharging current density, the higher the conductivity is. This means that the ohmic resistance of the 15 wt% WO_3/PFSA membrane is reduced under operation. Compared to the proton conductivity measured at freestanding state (see Table 2), it clearly shows an obvious improvement in the conductivity under dynamic process. This improvement in proton conductivity for the WO_3/PFSA membranes partially attributes to the spill-over effect of WO_3 during the hydrogen oxidation on Pt-based catalyst, results in a dynamic characteristic of the WO_3/PFSA membrane to increase the proton conductivity. The oxidation of hydrogen is a dehydrogenation process. The nascent hydrogen atom enters the WO_3 lattice to form conducting, blue hydrogen tungsten bronze and consequently increases the conductivity of the membrane [14,15]. The formation of the hydrogen tungsten bronze increases the electronic channels in the membrane which equals to reduce the thickness of the membrane. As we known that if simply reduces the thickness of the membrane will loss its mechanical strength. The better performance of the 15 wt% WO_3/PFSA membrane than that of the 8 wt% WO_3/PFSA membrane can be explained mainly due to the formation of the continuous electronic channels. Additional evidence of the spill-over effect on the WO_3/PFSA membranes is that the membrane shows blue in color after polarization.

Table 2
Water uptake for different membranes

Samples	Water uptake wt% (room temperature)
3 wt% WO_3	18.7
5 wt% WO_3	20.1
8 wt% WO_3	21.4
15 wt% WO_3	21.1
Nafion® 112	17.3

4. Conclusion

The results showed that the WO_3/PFSA membranes in single fuel cells have the lower resistances during the operation due to the spill-over effect than that of the single fuel cell using Nafion® 112 membrane. It is revealed that the performances of the single cells with WO_3/PFSA membranes are superior to that of the single cell with Nafion® 112 membrane. This work opens a new way to reduce the resistance of the membrane in PEMFCs by adding active fillers which show a dynamic characteristic to increase the membrane conductivity during the fuel cell operation. It is extremely important for the fuel cells operating at high current densities since the lower membrane resistance results in lower voltage loss.

Acknowledgements

The authors gratefully acknowledge the support by the NSF of China (20476108), and the Guangdong Science and Technology Key Project (2007A010700001).

References

[1] S. Gottesfeld, T. Zawodzinski, Adv. Electrochem. Sci. Eng. 5 (1997) 195.
[2] K. Kanamura, T. Mitsui, H. Munakata, Chem. Mater. 17 (2005) 4845.
[3] J.D. Halla, M. Mamak, D.E. Williams, G.A. Ozin, Adv. Funct. Mater. 13 (2003) 133.
[4] A.B. Bourlinos, K. Raman, R. Herrera, Q. Zhang, L.A. Archer, E.P. Giannelis, J. Am. Chem. Soc. 126 (2004) 15358.
[5] C.N. Li, G.Q. Sun, S.Z. Ren, J. Liu, Q. Wang, Z.M. Wu, H. Sun, W. Jin, J. Membr. Sci. 272 (2006) 50.
[6] M. Aparicio, F. Damay, L.C. Klein, J. Sol-Gel Sci. Technol. 26 (2003) 1055.
[7] D. Kim, M.A. Scibioh, S. Kwak, I.H. Oh, H.Y. Ha, Electrochem. Commun. 6 (2004) 1069.
[8] R.C. Jiang, H.R. Kunz, J.M. Fenton, J. Membr. Sci. 272 (2006) 116.
[9] D.H. Jung, S.Y. Cho, D.H. Peck, D.R. Shin, J.S. Kim, J. Power Sources 106 (2002) 173.
[10] K. Vallé, P. Belleville, F. Pereira, C. Sanchez, Nat. Mater. 5 (2006) 107.
[11] R. Zeng, Y. Wang, S.L. Wang, P.K. Shen, Electrochim. Acta 52 (2007) 3895.
[12] X.L. Wei, P.K. Shen, Electrochem. Commun. 8 (2006) 293.
[13] R.B. Levy, M. Boudart, J. Catal. 32 (1974) 304.
[14] B.S. Hobbs, A.C.C. Tseung, Nature 222 (1969) 556.
[15] B.S. Hobbs, A.C.C. Tseung, J. Electrochem. Soc. 120 (1973) 766.
[16] P.K. Shen, A.C.C. Tseung, J. Electrochem. Soc. 141 (1994) 3082.
[17] A.C.C. Tseung, P.K. Shen, K.Y. Chen, J. Power Sources 61 (1996) 223.
[18] C.L. Gardner, A.V. Anantaraman, J. Electroanal. Chem. 449 (1998) 209.
[19] C.H. Lee, H.B. Park, Y.M. Lee, R.D. Lee, Ind. Eng. Chem. Res. 44 (2005) 7617.
[20] Z. Xie, C.J. Song, B. Andreaus, T. Navessin, Z.Q. Shi, J.J. Zhang, S. Holdcroft, J. Electrochem. Soc. 153 (2006) E173.
[21] J.R. Varcoe, R.C.T. Slade, G.L. Wright, Y.L. Chen, J. Phys. Chem. B 110 (2006) 21041.
[22] T.J.P. Freire, E.R. Gonzalez, J. Electroanal. Chem. 503 (2001) 57.
[23] V.A. Paganin, C.L.F. Oliveira, E.A. Ticianelli, T.E. Springer, E.R. Gonzalez, Electrochim. Acta 43 (1998) 3761.
[24] K.T. Adjemian, R. Dominey, L. Krishnan, H. Ota, P. Majsztrik, T. Zhang, J. Mann, B. Kirby, L. Gatto, M. Velo-Simpson, J. Leahy, S. Srinivasan, J.B. Benziger, A.B. Bocarsl, Chem. Mater. 18 (2006) 2238.